Lab on a Chip

Pericytes and shear stress each alter the shape of a self-assembled vascular network

Journal:	*Lab on a Chip*
Manuscript ID	LC-ART-07-2022-000605.R2
Article Type:	Paper
Date Submitted by the Author:	23-Nov-2022
Complete List of Authors:	Fujimoto, Kazuya; Kyoto University, Department of Microengineering; Kyoto University Erickson, Scott; Kyoto University, Nakayama, Masamune; Kyoto University, Ihara, Hroki; Kyoto University, Department of Micro Engineering Sugihara, Kei; Kyushu Daigaku, Department of Basic Medicine Nashimoto, Yuji; Kyoto University, Department of Microengineering; Tokyo Medical and Dental University, Institute of Biomaterials and Bioengineering Nishiyama, Koichi; Miyazaki Daigaku, Medical Science Miura, Takashi; Kyushu Daigaku, Medical Sciences Yokokawa, Ryuji; Kyoto University, Department of Microengineering; Kyoto University

ARTICLE

Pericytes and shear stress each alter the shape of a self-assembled vascular network

Kazuya Fujimoto,[a] Scott Erickson,[a] Masamune Nakayama,[a] Hiroki Ihara,[a] Kei Sugihara,[b] Yuji Nashimoto,[†a] Koichi Nishiyama,[‡c] Takashi Miura,[b] and Ryuji Yokokawa*[a]

Received 00th January 20xx,
Accepted 00th January 20xx

DOI: 10.1039/x0xx00000x

Blood vessel morphology is dictated by mechanical and biochemical cues. Flow-induced shear stress and pericytes both play important roles, and they have previously been studied using on-chip vascular networks to uncover their connection to angiogenic sprouting and network stabilization. However, it is unknown which shear stress values promote angiogenesis, how pericytes are directed to sprouts, and how shear stress and pericytes affect the overall vessel morphology. Here, we employed a microfluidic device to study these phenomena in three-dimensional (3D) self-assembled vasculature. Computational fluid dynamics solver (COMSOL) simulations indicated that sprouts form most frequently at locations of relatively low shear stresses (0.5–1.5 dyn/cm^2). Experimental results show that pericytes limit vascular diameter. Interestingly, when treated with imatinib or crenolanib, which are chemotherapeutic drugs and inhibitors of platelet-derived growth factor receptor β (PDGFRβ), the pericyte coverage of vessels decreases significantly but vessel diameter remained unchanged. This furthers our understanding of the mechanisms underlying vascular development and demonstrates the value of this microfluidic device in future studies on drug development and vascular biology.

Introduction

The microvasculature is composed of the smallest blood vessels (<100 µm), which pervade every tissue of the body and are thus relevant to a multitude of diseases. In tumors, excess growth factors form abnormal and inefficient vasculature, which hampers chemotherapeutic delivery but makes it easier for cancer cells to enter the bloodstream and metastasize.[1, 2] Wound healing depends on the formation of new vessels from pre-existing ones, a process termed angiogenesis.[3, 4] In both of these cases, microvasculature morphology and function is dictated by both physical and biological factors.

The most influential physical component regulating vascular morphology is shear stress on the vessel walls. Several mechanisms are involved; however, one of the primary contributors is mechanotransduction via the platelet endothelial cell adhesion molecule (PECAM-1, or CD31) in endothelial cells (ECs).[5] Additionally, the release of nitric oxide (NO), which regulates blood flow via vessel dilation, has been shown to regulate angiogenesis in response to shear stress.[6, 7] Knockout mice with a dysfunctional NO pathway also have impaired wound healing and angiogenesis.[3] The normal range of shear stresses in vessels can vary widely (10–70 dyn/cm^2), and the combination of shear stress mechanotransduction, NO signaling, and other mechanisms may lead to either increased or decreased sprouting under these shear stresses.[5] Therefore, studying the cumulative effect of these factors on vessels in a controlled *in vitro* system is useful as it enables us to study which shear stress values cause the greatest change in vessels.

Pericytes, the primary vascular support cells, are largely recruited by ECs via platelet-derived growth factor (PDGF). During vessel formation, ECs release PDGF-B, one of the three PDGF isoforms, which binds to PDGF receptor β (PDGFRβ) on the pericyte membrane. This binding event triggers changes in gene expression within the pericyte, altering cytoskeletal arrangement and leading to pericyte migration up the PDGF-B gradient toward ECs.[8, 9] When in contact with ECs, pericytes provide several supportive functions. Pericytes themselves produce vascular endothelial growth factor (VEGF), which increases EC survival.[10] Ang-1, an angiogenic growth factor of the angiopoietin family, is also produced by pericytes and localizes to the tip cells of vessel sprouts, suggesting an important role in sprout formation.[11] Ang-1 also decreases vessel permeability, countering the leak-inducing effect of VEGF.[12] As new sprouts form, the extracellular matrix (ECM) is degraded, which forms a tunnel into which the sprouts extend.[13] Pericytes are recruited by following these tunnels, depositing critical basement membrane proteins along the way, which structurally support ECs.[13] Pericytes can also contract, giving them a mechanical role in regulating vessel diameter and blood pressure, particularly in the brain.[14] Pericytes have also been shown to limit the growth of ECs once in contact.[15]

[a] Department of Micro Engineering, Kyoto University, Kyoto, Japan.
[b] Graduate School of Medical Sciences, Kyushu University, Fukuoka, Japan.
[c] International Research Center for Medical Sciences (IRCMS), Kumamoto University, Kumamoto, Japan
[†] Current affiliation: Institute of Biomaterials and Bioengineering, Tokyo Medical and Dental University, Tokyo, Japan.
[‡] Current affiliation: Department of Medical Sciences, University of Miyazaki, Miyazaki, Japan.
*Email: yokokawa.ryuji.8c@kyoto-u.ac.jp

In mice, tumor vasculature was shown to have irregular pericyte coverage and gene expression.[1] Metastasis is largely facilitated by leaky tumor vasculature, which allows cancer cells to enter the bloodstream more easily.[2] Until now, the relationships between PDGF signaling, pericyte coverage, and vessel morphology have only been studied in mouse models, which show changes in vessel morphology due to decreased pericyte coverage.[16, 17]

The effects of shear stress and pericytes on vascular morphology have often been studied *ex vivo* or in mouse models. However, *in vitro* models from human cells are being increasingly developed as alternatives. In one example, a two-dimensional (2D) EC layer on a gel surface was used to test the effects of shear stress on sprouting.[6] Using this system, it was found that shear stress-mediated sprouting is dependent on NO signaling. In another study, a multi-channel device was used to test the effects of a range of shear stress values on 2D EC monolayers.[18] However, these 2D assay systems do not recapitulate the 3D vessel structure and thus fall short in studying the effects of shear stress and pericytes on vessel shape. Previously, a system has been developed that facilitates the growth of a 3D network of self-assembled perfusable vasculature.[19] Since then, similar systems have been used to model cancer, the blood-brain barrier, and the effects of pericytes on the protein expression of vasculature.[20-22]

In this study, we aimed to use *in vitro* self-assembled vasculature to study the effects of shear stress and pericytes on vasculature shape. We first used the system to test several shear stresses and found that most sprouting occurred at locations of low shear stress. The results also showed that vascular morphological parameters such as the number of branches, endpoints, and junctions increase with shear stress. We then used the system to test the effects of pericytes and found that pericytes limit vessel diameter. Finally, we focused on the role of PDGF signaling in this effect. Treatment with two different inhibitors of PDGFRβ resulted in significantly decreased pericyte coverage, but the vessel diameter remained unchanged. Ultimately, this work improves our understanding of how shear stress and pericytes affect vasculature morphology while showing the promise of this system in advancing research into basic biology and drug development.

Methods

Microfluidic device fabrication

A 100 μm layer of SU-8 3050 (MicroChem, Westborough, MA, USA) was spin-coated on a Si substrate, exposed to UV light through a photomask, and then developed. A polydimethylsiloxane (PDMS; Sylgard 184, Dow Corning Toray, Tokyo, Japan) elastomer and curing agent were mixed at a 10:1 ratio and poured onto the substrate. PDMS was cured, removed from the substrate, and 2 mm ports were punched at the ends of each channel. PDMS and glass coverslips were treated with plasma and irreversibly bonded. The devices were sterilized with UV light for 1 hour before cell seeding.

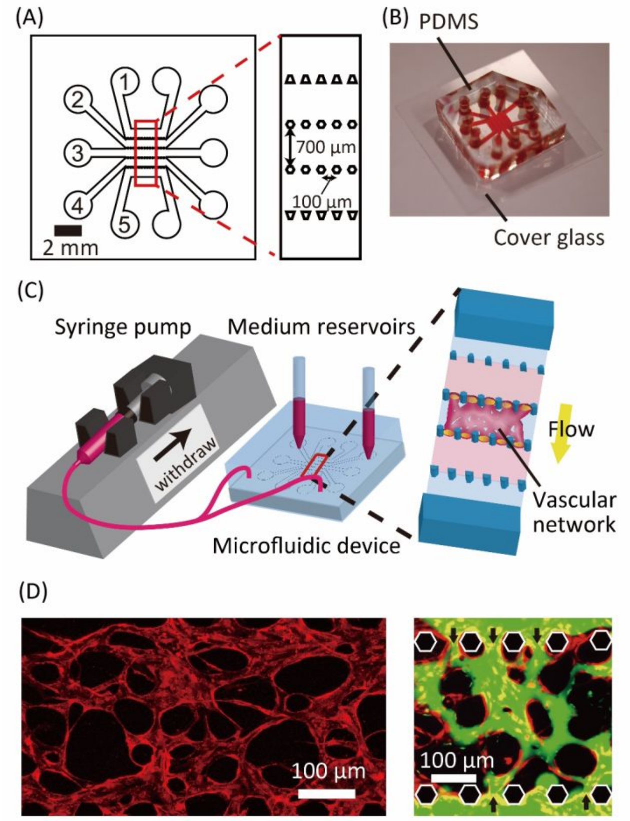

Figure 1: Device design and perfusion setup. (A) The five-channel device layout with channel numbers as indicated (left) and a complete device with red ink in the channels (right). (B) Perfusion setup whereby medium is drawn from reservoirs through the vessels that span the center channel. (C) Self-assembled vasculature (red) and perfusion with 70 kDa FITC-dextran (green). Black arrows indicate lumen openings.

Cell culture, device seeding, and PDGFR inhibitor treatment

Cells were initially cultured in culture flasks in a humidified 5% CO_2 incubator at 37 °C: red fluorescent protein expressing human umbilical vein endothelial cells (RFP-HUVECs; Angio Proteomie, Boston, MA, USA) in endothelial growth medium-2 (EGM-2; Lonza, Basel, Switzerland), green fluorescent protein-expressing human placental microvascular pericytes (GFP-pericytes; Angio Proteomie) in pericyte growth medium (super-rich formulation; PGM; Angio Proteomie) on a dish coated with Quick Coating Solution (Angio Proteomie), and human lung fibroblasts (hLFs; Lonza) in fibroblast growth media (Lonza).

After reaching 80% confluency, the RFP-HUVECs were removed with trypsin, centrifuged (1000 rpm for 1 min), and resuspended in a gel made up of 2.5 mg/mL fibrinogen (Sigma-Aldrich, St Louis, MO, USA), 0.2 mg/mL collagen (Corning, Corning, NY, USA), 0.15 U/mL aprotinin (Sigma-Aldrich), and 0.5 U/mL thrombin (Sigma-Aldrich), prepared in phosphate-buffered saline (PBS) on ice at 8×10^6 cells/mL. For devices with pericytes, RFP-HUVECs and GFP-pericytes were combined before centrifugation to reach a final GFP-pericyte concentration of 4×10^5 cells/mL (20:1 RFP-HUVECs:GFP-pericytes). Extra RFP-HUVECs were replated in EGM-2 for use on day 2. Separately, the LFs were removed from culture plates with trypsin and suspended in an identical fibrin–collagen gel at 5×10^6 cells/mL. The suspensions were kept on ice while injecting into the devices. The RFP-HUVEC/GFP-pericyte suspension was loaded into channel 3, and the LFs were loaded into channels 1 and 5. The devices were incubated at 37 °C and 5% CO_2 for 20 min during gel polymerization. Channels 2 and 4 were filled with EGM-2. Two days later, the replated RFP-HUVECs were removed with trypsin and resuspended in EGM-2 at 5×10^6 cells/mL. The medium was removed from channel 2, and this cell suspension was injected. The devices were then turned 90° to allow the RFP-HUVECs to settle toward channel 3, and the devices were placed in an incubator for 30 min. The same was performed for channel 4. Thus, the outer surfaces of channel 3 were coated with RFP-HUVECs to promote lumen opening to channels 2 and 4.

Imatinib mesylate (imatinib; Cayman Chemical, Ann Arbor, MI, USA) solid and crenolanib (Abcam, Cambridge, UK) solid were dissolved in dimethyl sulfoxide (DMSO) to 10 mg/mL and 1 mg/mL, respectively, and then added to EGM-2 to reach a final concentration of 25 and 1 μM, respectively. For all devices, 50% of the medium volume was changed daily with EGM-2. Imatinib and crenolanib were administered to the appropriate devices from day 3, which ensured that the drugs did not prevent the formation of vessels.

Perfusion setup

A syringe pump (KDS 210, KD Scientific, Holliston, MA, USA) was connected to the ports of channel 2 and 1 mL micropipette tips were filled with media and inserted into the ports of channel 4 to serve as media reservoirs. The pump withdrew media at 0, 10, 30, 60, or 120 μL/h from the reservoirs and through the vessels in

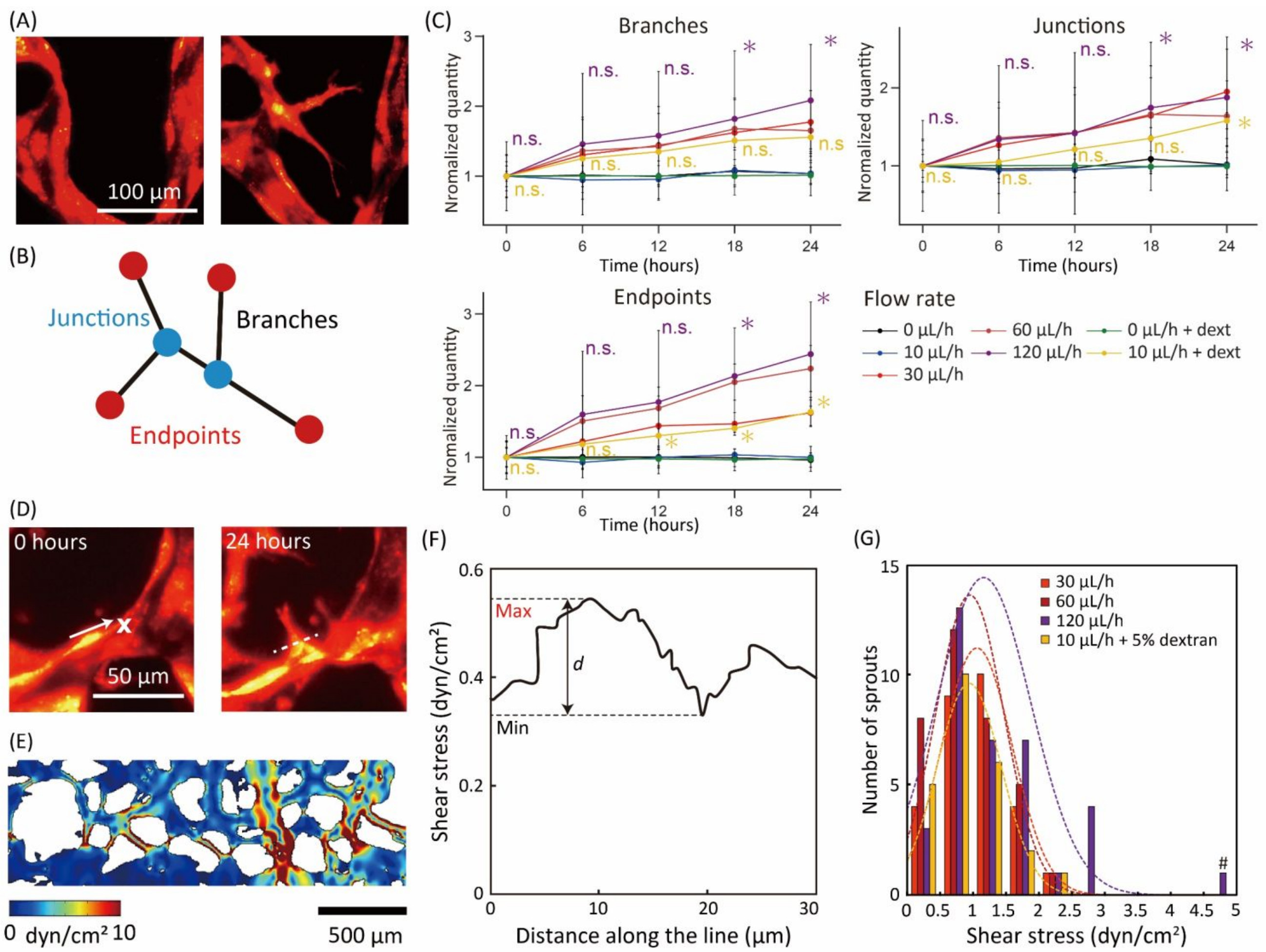

Figure 2: Shear stress affects vessel morphology. (A) Example of sprout formation after 24 hours of flow. (B) Definition of vessel morphological parameters. (C) The number of branches, endpoints, and junctions during 24 hours of flow, including high viscosity medium with dextran. Data represent mean ± standard deviation (S.D.) from more than three individual devices. Statistical significance of the flow rates effect on the paramters was determined by one-way ANOVA for each time point and Dunnett's test for each flow rate. The * ($p<0.05$) indicates a significant difference between the 120 uL/h (purple) and 0 uL/h conditions. Statistical significance of the dextran effect was determined by t-test between the 10 μL/h + dextran condition (yellow) and 10 μL/h condition (blue; *$p < 0.05$). (D) Fluorescence images showing sprout formation. For each sprout, shear stress is extracted along a manually drawn dashed line. (E) Contour plot of shear stress by COMSOL simulation. (F) Shear stress along the dashed line shown in (D) at time 0. The maximum shear stress value at each sprouting location was used for (G). (G) Histogram indicating the number of sprouts formed at each shear stress. Dotted curves represent Gaussian distribution. The bin size of 0.5 dyn/cm² was chosen based on the difference between minimum and maximum shear stress values, *d*, shown in (F). The rightmost bar marked with # represents the cumulative number of sprouts with a shear stress larger than 4.74 dyn/cm². All data were taken from > three replicate devices.

channel 3. A high-viscosity medium was prepared by adding 5% (w/v) dextran (150 kDa; Sigma-Aldrich) to EGM-2. Viscosities were measured by a viscometer (VM-1G, SEKONIC, Tokyo, Japan), with high-viscosity medium (4.03–4.04 mPa·s) being approximately four times more viscous than the standard medium (0.94–0.95 mPa·s) at 37 °C.[23]

Imaging and vessel analysis

For perfusion experiments, an inverted microscope (CKX41, Olympus, Tokyo, Japan) was used to obtain fluorescence images every 6 hours for 24 hours to capture the shape of the vessels. For long-term (13 day) vessel analysis, a z-stack of images with a 2.7-µm step size was captured for the entire thickness of the vessels, with two regions of interest (ROIs) per device every other day using laser scanning confocal microscopy (FluoView FV3000, Olympus) (Fig. S1).

All analyses of vessel morphological parameters and pericyte coverage were performed using ImageJ (NIH). A maximum intensity z-projection was performed for each channel (RFP and GFP), which was then filtered for noise and binarized. Disconnected points in the vasculature were automatically removed. Binary images of the vasculature were then skeletonized and analyzed for the number of endpoints, junctions, and branches. The average vessel diameter was calculated by dividing the total binarized vascular area by the total skeleton length and total number of branches. The values were normalized to the initial time point. To calculate pericyte coverage, the image calculator function of ImageJ was used to perform the AND operation on the binarized z-projections of the RFP and GFP channels. The total area of the resulting image was divided by that of GFP for normalization. Therefore, a value of 1 indicates that all pericytes are overlapping vessels, whereas a value of 0 indicates that there is no overlap and pericytes exist only in the spaces between vessels.

Computational fluid dynamics simulation and plotting of shear stress values

The 2D projections of vessel geometry at the initiation of flow (t = 0 hours) acquired by the image processing explained above were imported into a computational fluid dynamics solver (COMSOL Multiphysics ver. 5.1). The fluid dynamic parameters were estimated using the finite element method. The solver was set to solve the Navier–Stokes equation assuming laminar, time-independent, and incompressible flow. The vessels were assigned a uniform height of 10 µm (with a rectangular cross section instead of ellipsoidal; justification provided in Fig. S2A and later in the text) and a no-slip boundary was adopted for all vessel walls, except for the openings to channels 2 and 4. The volume flowing from channel 2 was constant (10–120 µL/h). The pressure of channel 4 was set to the hydrostatic pressure of the medium reservoir (200 Pa). Shear stress (τ) was calculated using the following equation:

$$\tau = \mu \partial u / \partial y$$

where μ is the viscosity of the medium (0.95 and 4.04 mPa·s for normal and high-viscosity media, respectively), u is the velocity, and y is the distance from the vessel wall.

In the fluid dynamics simulation, we approximated the vessel geometry in 2D and set the height as 10 µm for all vessels. Since the actual height of vessels varies slightly, these approximations do induce an error. To assess the error, we determined the average height of the vasculature (17.9 ± 8.1 µm (n = 10)) and calculated the normalized shear stress and relative error of shear stress (SI text, Fig. S2). The relative error increases to 0.5

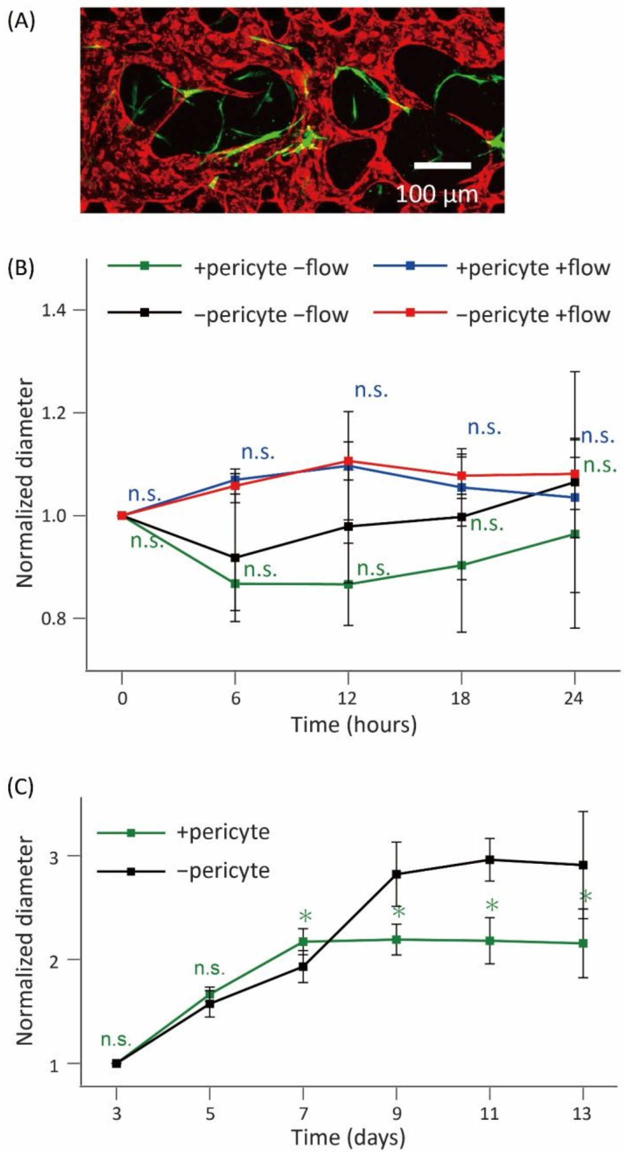

Figure 3: Pericytes affect vessel morphology in the long term. (A) Representative fluorescence image of pericyte-wrapped vessels. Red, RFP-HUVECs; green, GFP-pericytes. (B) Plot showing little effect of pericytes on vessel diameter over 24 hours (experiment done with or without flow). Statistical significance of the pericyte effect without flow was determined by t-test between +pericyte−flow (green) and −pericyte−flow (black). The effect with flow was also tested between +pericyte+flow (blue) and −pericyte+flow (red). (C) Plot showing considerable effect of pericytes on vessel diameter over 13 days (experiment done without flow). All data were taken from more than three individual devices. Plots represent mean ± standard deviation (S.D.). *p<0.05. All data were taken from > three replicate devices.

when an original 50-µm width vessel with a height of 25 µm was assumed to have a height of 10 µm, which means the shear stress may be overestimated by up to 50%. However, the range of shear stresses reported here vary over an order of magnitude (Fig. 2G), so we can sufficiently estimate the sprout-inducing shear stress values and compare with previous studies. More details are discussed in the discussion section.

Fluorescence images acquired before and after flow were compared to determine the location of sprouting. Using the simulation output, lines were drawn across the base of each future sprout and the maximum shear stress along the lines was extracted. This was performed for all sprouts in three ROIs (minimum 28 sprouts in total) for the four flow conditions that showed significant sprouting: 30, 60, and 120 µL/h, and 10 µL/h with dextran. A histogram with a 0.5 dyn/cm^2 bin size was created for all sprouts. Assuming a normal distribution, Gaussian fitting was performed for each condition. The shear stress of 4.74 dyn/cm^2 (120 µL/h) was greater than three times the standard deviation from the mean and was therefore deemed an outlier not to be considered in the Gaussian fit.

2D migration assay setup and imaging

A simple aluminum mold was custom made to produce PDMS pieces with two chambers of 5 mm height and separated by a 2 mm-thick wall. PDMS was prepared as previously described. Each PDMS piece was sterilized by UV for one hour before use. RFP-HUVEC and GFP-pericyte cultures were initiated as previously described before suspending each separately in EGM-2 (Lonza) to reach 3×10^5 cells/mL. A 6-well cell culture plate was then prepared by coating with Quick Coating Solution (Angio Proteomie). A two-well PDMS piece was then manually pressed into the bottom of each well. Adhesion between PDMS and the culture plate was sufficient to hold media in the two rectangular chambers. The RFP-HUVEC and GFP-pericyte suspensions (0.5 mL) were each added to their own chamber and allowed to settle for 1 hour.

Imatinib and crenolanib media were prepared as previously described. To account for the possible effect of DMSO on pericyte migration, an identical DMSO concentration (0.27%) was used in the control. EGM-2 with imatinib and crenolanib was prepared every other day to avoid precipitation of the inhibitors.

After the cells settled, PDMS pieces were carefully removed, the wells were washed three times with PBS, and EGM-2 was added to each well with 25 µM imatinib, 1 µM crenolanib, or without an inhibitor. The gap between cell populations was immediately imaged by confocal microscopy. The locations were saved by the mechanical stage, and three images were recorded for each well every 12 hours. ImageJ was used to count cells in the gap at each time point, normalized to the initial count.

Time-lapse imaging

Time-lapse images of pericytes in devices with imatinib, crenolanib, or without an inhibitor were captured to observe short-term pericyte migration. A stage-top incubator (Inub-Onics-F1-MX, TokaiHit, Shizuoka, Japan) was placed on the confocal microscope stage and prepared prior to placing the devices inside. The stage heater was set to 42 °C, the incubator top heater was set to 38 °C, and the mixed gas (N_2, O_2, and CO_2) flow rate was calibrated to 16 mL/min. Twelve days after seeding, one device with imatinib and one control device were placed in the incubator, and two ROIs per device were recorded by the mechanical stage. Z-stacks were collected automatically at a 2.7-µm step size every 30 min for 15 h. Using ImageJ, a maximum z-projection was performed on the GFP (pericyte) channel at each time point. Projections were then color-coded by time and superimposed to create a single image. These images were assessed qualitatively for instances of directed GFP-pericyte migration, which appeared as an ordered gradient of color.

Immunostaining

Devices were prepared for staining on day 14 of culture by removing all media, washing thoroughly with PBS (channels 2 and 4), and adding 4% paraformaldehyde (PFA) to all channel openings. After 30 min at room temperature (RT; 20–25 °C), the PFA was removed, and the devices were washed thoroughly with PBS. The devices were then treated with 0.05% Triton X-100 (Sigma-Aldrich; diluted in PBS) for 10 min, washed, and then blocked with 10% donkey serum for 2 hours at RT. The primary antibodies used were rabbit anti-PDGFRβ (Abcam 32570; 1:100) and rabbit anti-PDGF-B (Abcam 23914; 1:500), each diluted in blocking buffer, and applied for 14 hours at 4 °C. After washing thoroughly, the secondary antibody, donkey anti-rabbit Alexa Fluor 647 (A31573, Thermo Fisher, Waltham, MA, USA; for both PDGFRβ and PDGF-B) was diluted 1:400 in PBS and applied for 2 hours at RT. The nuclei were stained with DAPI (D371, Thermo Fisher; 1:2000) during the secondary antibody incubation. The negative control was treated the same, but without a primary antibody. Confocal images were obtained within 24 hours at 40× magnification and a 1-µm step size.

Statistical analysis

All vessel parameter data are presented as the mean ± standard deviation (S.D.) for at least three regions of interest taken from more than 3 replicate devices, as indicated. Shear stress values were obtained for all sprouts in the three ROIs for each flow condition.For the assessment of flow rate effect, one-way ANOVA was used to determine whether or not the difference between values at each timepoints were statistically significant. Then, at each time point showing significance by ANOVA, Dunnett's test was performed to determine statistical significance of the difference between the values taken from each flow rate and control (0 μl/h) at each time point assessed signifificant by one-way ANOVA. Two-tailed t-test was used for other cases, with $p < 0.05$ considered statistically significant.

Results

Shear stress changes vessel morphological parameters

We used a previously established 5-channel microfluidic device that allows the self-assembly and perfusion of the vasculature (Fig. 1A and B).[19, 20] The outer channels (channels 1 and 5)

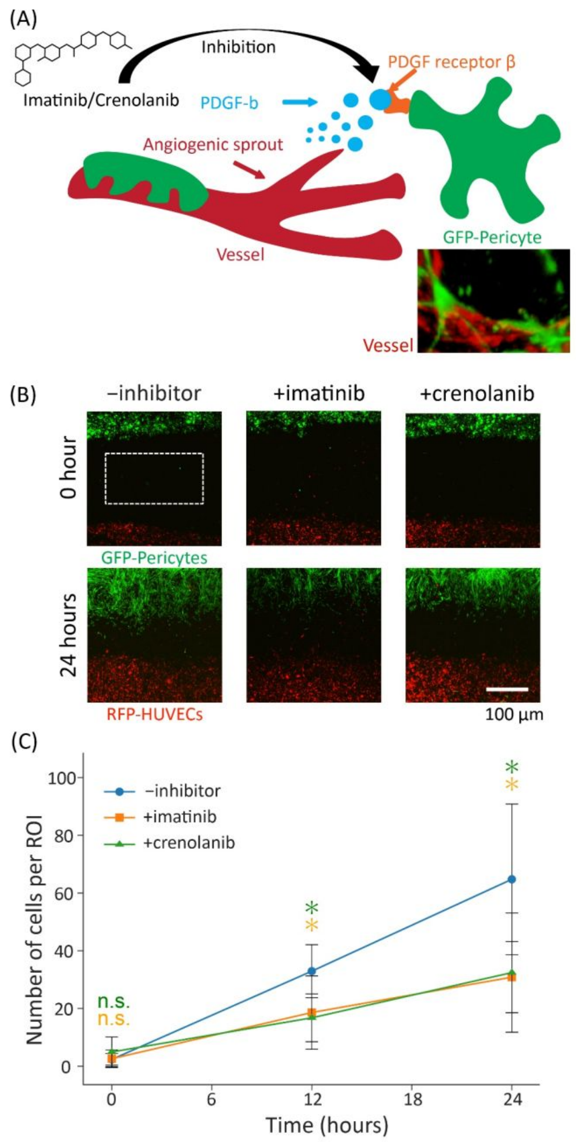

Figure 4: Inhibitors impact pericyte migration. (A) Schematic showing endothelial cells releasing platelet-derived growth factor (PDGF)-b, which binds to platelet-derived growth factor receptor β (PDGFRβ) on pericytes. Imatinib and crenolanib inhibit PDGFRβ. (B) 2D assay showing the effect of imatinib and crenolanib on cells over 24 hours. An ROI (dashed white line) is set for counting. (C) The number of cells in the gap of the 2D assay. Data represent mean ± standard deviation (S.D.) of six replicates of wells from two individual trials. Statistical significance was determined between −inhibitor (blue) and +imatinib (orange) and between −inhibtor and +crenolanib (green). *p<0.05. All data were taken from > three replicate devices.

contain hLFs, and the center channel (channel 3) contains RFP-HUVECs. hLFs secrete growth factors, including VEGF, which diffuse across the intermediate medium channels (channels 2 and 4) and support vessel formation in channel 3. Micro-posts separating the channels maintain cell/gel mixtures in the appropriate channels during seeding and facilitate lumens opening to channels 2 and 4. A perfusable microvascular network forms after approximately 4 days in culture. To induce flow, 1 mL micropipette tips were inserted into the two ports of channel 4 and filled with cell culture medium, serving as reservoirs, and a syringe pump was then connected to the two ports of channel 2 (Fig. 1B). The pump withdrew the medium from the reservoirs of channel 4 and through the vessels in channel 3, as shown by the 70 kDa FITC–dextran in Fig. 1C. After 4 days, we selected perfusable devices for further experiments. Approximately 60% of the devices were perfusable at this time point.

We observed changes in vessel morphology, including angiogenic sprouting, after subjecting to flow for 24 hours (Fig. 2A). To characterize the vessels and sprouting under different shear stresses, the number of branches, junctions, and endpoints were measured every 6 hours at five flow rates (0, 10, 30, 60, and 120 µL/h) using standard EGM-2 (Fig. 2B and C). The data show that the number of branches, junctions, and endpoints generally increased with the flow rate. Each parameter approximately doubled after 24 hours of flow at 60 and 120 µL/h, while the parameters increased by approximately 1.5 times after 24 hours of 30 µL/h flow. The increases were statistically significant compared to the parameters without flow (0 µL/h) (SI table 1). These values did not increase over time without flow (0 µL/h) or at a flow rate of 10 µL/h.

To determine whether this effect was due to shear stress or simply improved nutrient delivery, we used dextran to increase the viscosity of EGM-2 by four times and tested it at 0 and 10 µL/h. There was no difference between the high-viscosity and regular media at 0 µL/h for any of the morphological parameters (Fig. 2C), indicating that dextran did not negatively impact the cells. However, by using the high-viscosity medium at 10 µL/h, we observed an increased number of endpoints, junctions, and branches compared to using standard EGM-2 at the same flow rate. We therefore concluded that, independent of the flow rate, shear stress changes the vessels in the device.

Most angiogenic sprouts form at locations of low shear stress

Sprouting is a distinct feature of angiogenesis and has therapeutic potential in various diseases, including preeclampsia and cancer.[24] We observed angiogenic sprouting from existing vessels after medium flow for 24 hours (Fig. 2D). The shear stress applied to the vessel wall was calculated using COMSOL software (Fig. 2E). The simulation results were validated with contour plots of flow velocities and pressure to confirm that they represent the actual phenomena (Fig. S3). The resulting contour plot of the shear stress values was used to estimate the shear stress at the locations where sprouts would later form (within 24 hours of flow).

The maximum shear stress along the line drawn across the base of every future sprout was extracted (Fig. 2F), and it was found that these values were distributed in the range of 0–5 dyn/cm^2. Most of the sprouts, approximately 61%, formed at locations with shear stresses in the range of 0.5–1.5 dyn/cm^2 (Fig. 2G). The average shear stress at which sprouts form was nearly the same for each condition (0.9–1.2 dyn/cm^2), supporting the hypothesis that low shear stress values are favorable for sprouting. In this study, a bin size of 0.5 dyn/cm^2 was chosen for the histogram to represent all sprouting because the difference between the maximum and minimum shear stress values (labeled *d* in Fig. 2F) at each sprout location was considerably smaller than 0.5 dyn/cm^2.

Change of vessel diameters under flow were affected by pericytes

Pericytes regulate vessel diameter[14] and the vessel response to flow[25]; therefore, we evaluated whether they display this ability in our system. RFP-HUVECs and GFP-pericytes were co-cultured in the device at a ratio of 20:1. Because the proliferation of GFP-pericytes is higher than that of RFP-HUVECs, the final ratio of ECs to pericytes was comparable to that reported *in vivo* (7:1–9:1).[26] Co-cultured cells successfully developed into perfusable vasculature (Fig. 3A). After 6 days in the device, flow (30 μL/h) was initiated for 24 hours. Under these flow conditions, the normalized diameter of the vessels showed no significant difference with and without pericytes (Fig. 3B).

When cultured without flow for an extended period of 13 days, we observed that pericytes limited the expansion of vessel diameter (Fig. 3C). Without pericytes, the normalized diameter of the vessel increased until approximately day 9 when it was three times the initial (day 3) diameter. With pericytes, however, the normalized diameter plateaued around day 7 at twice the initial diameter. Although the short-term effects of pericytes on the normalized diameter of the vessels could not be observed, the platform proved useful for studying the effect of pericytes on long-term vessel development. Therefore, subsequent experiments were performed without flow and for at least 13 days.

Pericyte migration can be reduced in 2D by inhibiting PDGF signaling

PDGF signaling is a primary mechanism of pericyte recruitment by ECs (Fig. 4A). We hypothesized that inhibiting this pathway would decrease the effect of pericytes on vessel diameter. To confirm the relevant protein expression in the system, devices with RFP-HUVECs and GFP-pericytes were first immunostained for PDGF-B and PDGFRβ (Fig. S4). PDGFRβ was localized in pericytes, whereas PDGF-B staining was observed in both pericytes and HUVECs, with the strongest signal localized to HUVECs.

To test whether inhibition of the PDGF signaling pathway would reduce pericyte wrapping of vessels and thus affect the vessels, we used two inhibitors of PDGFRβ, imatinib and crenolanib. These chemotherapeutic drugs inhibit few tyrosine kinase receptors, including PDGFRβ (Fig. 4A), and have been previously studied as therapeutic inhibitors of pericyte function and vascular growth.[27] However, they have not been studied on vasculature *in vitro*.

We first developed a 2D assay in which two cell populations can be separated by 2 mm (Fig. 4B). By counting the number of cells in the gap over time, we can deduce their relative ability to fill the gap (an indicator of migration ability). This experiment was performed using EGM-2 with imatinib and crenolanib at IC_{30} concentrations of 25 μM and 1 μM, respectively.[28] Fluorescence images showed an evident difference in the ability of cells to fill the gap compared to the control (Fig. 4B). The number of cells per ROI significantly decreased with inhibitors after 12 and 24 hours (Fig. 4C). Based on these results, we tested these inhibitors in a 3D system.

Pericyte coverage of vessels is significantly reduced by the inhibitors

Based on the distinct effect of imatinib and crenolanib on pericyte migration after 24 hours in the simple 2D assay, we chose day 3 as the initial time point to apply inhibitors to allow sufficient vessel development before inhibiting pericyte recruitment. Fluorescence images captured on days 5 and 6 showed a clear qualitative difference in pericyte activity (Fig. 5A). Control devices (without an inhibitor) showed that pericytes effectively move toward and wrap vessels. However, devices with imatinib show that there are fewer pericytes and that they often move away from the vessels. Interestingly, this difference in pericyte activity was evident over the course of one day.

To further investigate the short-term activity of pericytes and their recruitment by PDGF signaling, a time-lapse image was acquired, and frames were color-coded and superimposed (Fig. S5). In the resulting images, directed pericyte motion appears as a linear color gradient. We hypothesized that pericytes with inhibited PDGF signaling would move randomly, rather than in a single direction. Indeed, we observed more instances of directed pericyte motion in the control devices than in the imatinib-treated devices, suggesting that pericytes move toward the vessels via PDGF signaling.

The effect of PDGF signaling inhibition was quantified by the GFP-pericyte coverage over the course of days 3–13 in devices with and without inhibitors. Coverage was calculated by quantifying the overlap of GFP and RFP channels relative to the total GFP after z-projection and binarization (Fig. 5B). By this method, coverage varies between 0 and 1, where a value of 0 indicates that pericytes exist only in the gaps between vessels and a value of 1 indicates that all pericytes are overlapping vessels. In the absence of any inhibitor, pericyte coverage gradually increases to 0.6 by day 11 (Fig. 5C). Interestingly, devices with imatinib and crenolanib exhibited pericyte coverage that consistently remains around 0.4 for the duration of the experiment (Fig. 5C). We thus concluded that the addition of PDGF signaling inhibitors reduces the ability of pericytes to locate and cover vessels.

Vessel morphology changes little despite inhibited pericyte coverage

Finally, we tested the effect of PDGFR inhibitors on vessel diameter, with the hypothesis that decreased pericyte coverage would change the pericytes' ability to regulate vessel diameter. The diameter was calculated on odd-numbered days for devices with and without inhibitor. Interestingly, the average vessel diameter under all three conditions (imatinib, crenolanib, and control) was nearly identical throughout the duration of the experiment (Fig. 5D, Fig. S6). This indicates that although pericyte coverage was reduced by approximately one-third, the pericytes' effect on diameter was unchanged. Notably, the vessel diameter was not affected by inhibitors when the vessels were cultured without pericytes (Fig. S7). This suggests that the inhibitors did not damage the vessels. Taken together, we report that pericytes limit vessel diameter, even with significantly reduced contact with vessels by PDGF inhibitors.

Discussion

This microfluidic device facilitates the self-assembly of HUVECs and pericytes into vessels, which are structurally similar to those *in vivo*. The system and analysis methods are robust, allowing the manipulation and study of complex physical and cellular interactions. Several biological systems depend on the regulation of vessel morphology. Here, we show that pericytes and shear stress are two important factors in this process.

Shear stress values in the body vary by location and vessel type, with shear stresses of 10–70 dyn/cm^2 and 1–6 dyn/cm^2 in arteries and veins, respectively.[23] The effect of shear stress on vessels is commonly studied in embryos[29] or simple *in vitro* systems, such as 2D cell layers.[6]

Sprout formation depends on shear stress, as reported in previous *in vitro* studies.[30, 31, 32] The shear stress that induces sprouting in our study was 0.5–1.5 dyn/cm^2, which is lower than that reported previously (3 to 10 dyn/cm^2).[30, 31, 32] Because we obtained shear stress using 2D images with a given height of 10 µm in COMSOL, we considered the difference of shear stress from previous studies was caused by the variation of vessel height. However, the evaluation of shear stress revealed that the shear stress would be overestimated by only up to 50% when the original vessel (with a height of 25 µm) was assumed to have a height of 10 µm (Fig. S2). Thus, the error introduced by the shear stress calculation cannot solely explain the difference from previous studies.

We can attribute the difference to several other factors. The most significant difference from previous studies is the method to form our 3D vessels. Previous studies utilized a pre-defined structure of ECM gel as a scaffold to form vessel structures,[30] which enables the analytical calculation of the shear stress based on fluid dynamics. In contrast, we used a self-assembled vascular network for the first time to investigate the relation between sprouts and shear stress (Fig. 2G).[31] This led to vessels

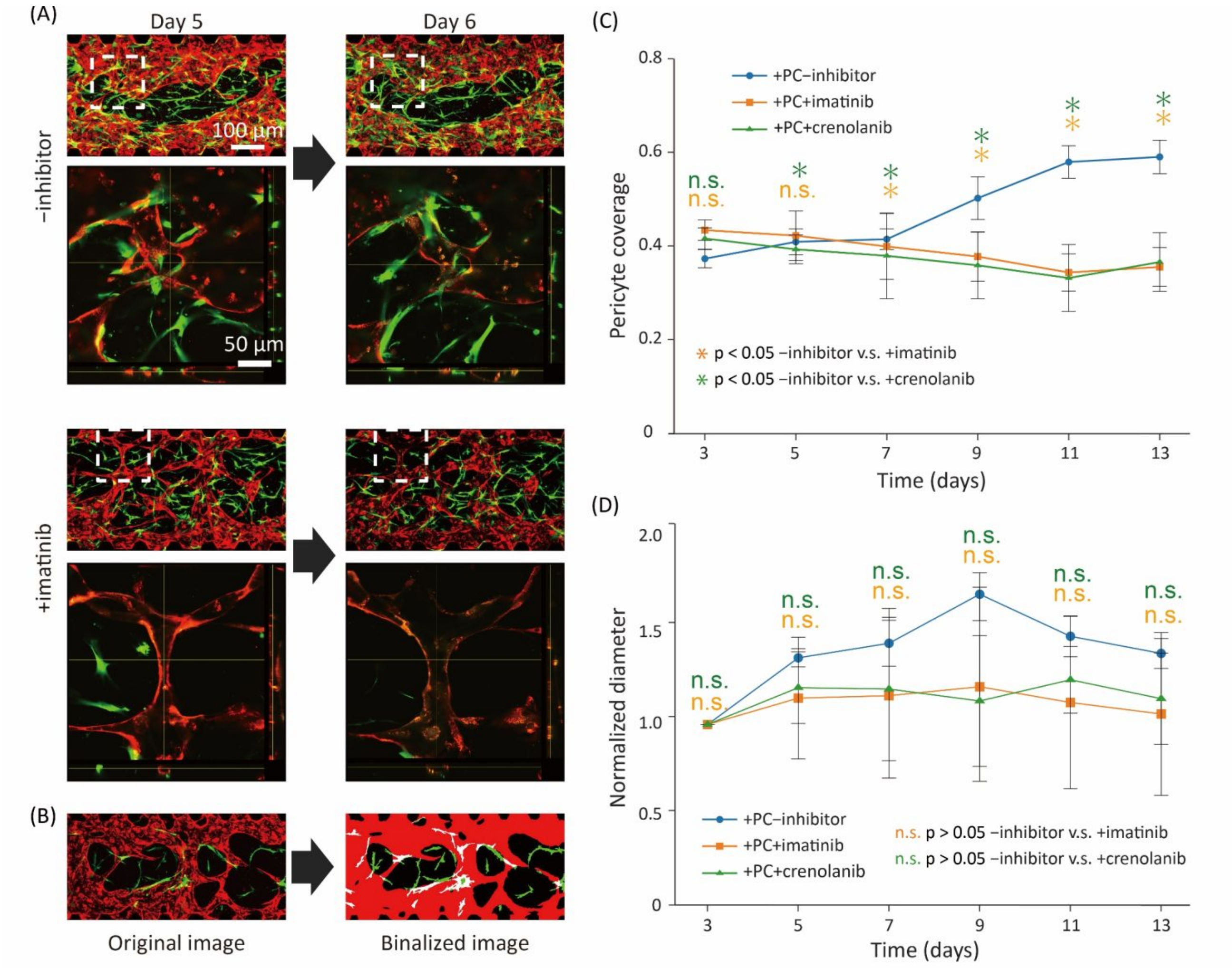

Figure 5: Inhibitors affect pericyte coverage of vessels. (A) Fluorescence images showing how imatinib appears to affect pericyte migration over 24 hours. Arrows indicate instances of pericyte wrapping in the 40× images captured on day 6. (B) Fluorescence image showing RFP-HUVECs (red) and GFP-pericytes (green) and binary images used to determine overlap between them (white). (C) Plot showing the impact of imatinib and crenolanib on pericyte overlap of vessels. (D) Plot showing vessel diameter with imatinib and crenolanib. Data represent the mean ± standard deviation (S.D.) of at least three replicates of devices. Statistical significance was determined between +PC−inhibitor (blue) and +PC+imatinib (orange), and between +PC−inhibitor and +PC+crenolanib (green). n.s. $p>0.05$ and *$p<0.05$. All data were taken from > three replicate devices.

that were shorter in height and had a greater variation in width than those in previous reports.[30, 31] The combined effect of other factors including ECM stiffness, interstitial flow, and HUVEC lot needs to be further explored to better understand the sprouting mechanism.[33]

The method proposed here is advantageous to investigate a wide range of shear stresses at a given flow rate, because the sizes of the self-assembled vessels vary and the shear stress differs depending on the size. In previous studies, shear stress could be tuned only by changing flow rate, due to a pre-designed straight channel.[30, 31, 32, 33] Here, regardless of flow rate, most sprouts formed at locations with low shear stress values, and all vessel parameters tended to increase with flow rate and viscosity (Fig. 2C). This suggests that even at the highest flow rate, the shear stresses that induce sprouts in our system were relatively low (Fig. 2G).

In addition to studying shear stress, self-assembled vessels also allow the study of more complex cell interactions and their effects on vessel shape *in vitro*. In the brain, pericytes have been shown to actively regulate vessel diameter by contracting in response to nervous stimuli, thereby controlling blood flow.[14] Previous in vitro experiments have shown that interaction between ECs and pericytes resulted in lower permeability of the vessel wall.[13, 22, 34] Here, the effect of flow on the morphology of the self-assembled vascular network with pericytes was investigated for the first time. We found that GFP-pericytes did not affect vessel diameter during 24 hours with media flow. Due to the technical limitations of the device, long-term flow experiments could not be performed. However, we demonstrated the ability of pericytes to regulate vessel diameter for 13 days in culture without flow, a phenomenon that is consistent with previous findings *in vitro* and *in vivo*.[13, 16, 22] Applying flow for a greater duration of time will provide a further understanding of the interaction between vasculature and pericytes.

PDGF signaling between ECs and pericytes is important for complete pericyte coverage of vessels. Previous studies on mice with defective PDGF signaling showed that vessel diameter increases due to a lack of pericytes.[16, 17] In the control condition (without inhibitors), the ratio of pericyte coverage was found to increase to approximately 0.6 after 13 days. By blocking PDGFRβ with imatinib or crenolanib, we showed that pericyte coverage is limited to a ratio of approximately 0.4 for the entire 13 days of analysis. This suggests that imatinib and crenolanib prevent pericytes from responding to PDGF-B gradients, causing them to move without direction and preventing them from covering vessels. It is known that PDMS absorbs/adsorbs hydrophobic molecules. Imatinib and crenolanib are hydrophobic molecules with a high estimated LogP value of 3.7 and 3.5, respectively, which indicates the hydrophobicity of the compounds. So, the effective concentrations in our device are likely decreased.[35, 36] However, a significantly smaller pericyte coverage ratio with the inhibitors (Fig. 5C) indicated that the effective concentrations were sufficiently high to block the PDGF signaling.

Despite the significantly reduced pericyte coverage, the vessel diameter remained unchanged, suggesting that pericytes can restrict vessel diameter even with only 40% coverage (Fig. 5D). This could be the effect of indirect pericyte support that does not require contact with vessels, such as through ECM protein secretion and maintenance, which are functions of pericytes that have been shown previously.[13] In any case, we found that reducing pericyte coverage is not necessarily enough to prevent their regulation of vessel diameter.

This work supports further studies on the relationships between vessel morphology, shear stress, and pericytes. In studies of tumor vasculature, for example, shear stresses have been used to guide mathematical models.[37, 38] Precise *in vitro* measurements of sprouting shear stress may be used to test and inform these models. Likewise, wound healing has been studied extensively both *in vivo* and *in silico*[4, 39] and could be studied further using *in vitro* systems capable of analyzing shear stresses. For instance, endothelial nitric oxide synthase (eNOS) largely dictates angiogenesis in response to shear stress.[7] Mice without eNOS have considerably reduced capacity for wound healing.[3] The effect of eNOS on shear stress and angiogenesis could be further studied *in vitro*, where the role of pericytes could also be explored.

We used a microfluidic system to test a range of shear stresses and found that most sprouting occurred at locations with low shear stresses. The results also showed that morphological parameters of vasculature such as the number of branches, endpoints, and junctions increase with shear stress. We then used the system to test the effects of pericytes and found that pericytes limit vessel diameter. Finally, we focused on the role of PDGF signaling in this effect. By inhibiting PDGFRβ with the chemotherapeutic drugs imatinib and crenolanib, we showed that GFP-pericyte coverage was significantly decreased, but vessel diameters were not affected. Ultimately, this work deepens our understanding of how shear stress and PDGF signaling affect vessel morphology, while showing the promise of these devices in advancing research into basic biology and drug development.

Here, we focused on how pericytes change vasculature during long-term culture. However, these methods may also be used to explore their active roles in vasoconstriction. Pericytes contract and dilate in response to neurotransmitters and electrical stimulation both *ex vivo* and *in vivo*, thereby modulating blood flow.[40, 41] By adding neurotransmitters to the vasculature, *in vitro* vessel morphology and pericyte coverage could be tracked via time-lapse images recorded on the scale of minutes, and the contractile action of pericytes could be observed. Analyses of shear stress and sprouting could also be used to characterize changes in the vessels. This could support *in vivo* experiments by providing a platform to study the yet-unclear role of pericytes in stroke pathogenesis.[42, 43]

Toward the future studies discussed above, the experimental methods reported here have three main issues: the limited volume of reservoirs, indirect estimation of shear stress, and the number of devices per experimental batch. Because the media in the reservoir was withdrawn by a syringe pump, the volume can support up to 24 hours and refilling of media is necessary for long-term experiments. For shear stress, we used numerical simulation to estimate the values, leaving uncertainty in matching with actual values. Direct measurement of these parameters will provide us more reliable understanding. For flow conditions, the maximum number of devices that we can handle per batch is six. Therefore, arraying devices and pumps is necessary to increase throughput, which would thus enable us to simultaneously evaluate the combined effects of intraluminal or interstitial flow, pericytes, and biochemical inhibitors and activators.

Conclusions

Using a microfluidic device to grow self-assembled vasculature, we demonstrated the effects of shear stress and pericytes on blood vessel morphology. Simulations of shear stress in vessels allowed us to determine that most sprouting (61% of sprouts) occurred at locations with shear stresses in the range of 0.5–1.5 dyn/cm^2. We then added pericytes to the system and showed that they significantly decreased the vessel diameter.

The addition of PDGF signaling inhibitors resulted in a significant reduction in pericyte coverage of the vessels compared to the control devices. Despite this decreased coverage, the vessel diameter remained equal to that in the control devices without inhibitors, indicating that pericytes can regulate vessel diameter even with reduced coverage. We have two hypotheses to explain this phenomenon. One is that pericytes only require a small coverage ratio to limit diameter; the other is that pericytes may limit vessel diameter indirectly, such as through the production of signaling molecules or ECM proteins.

Together, these results provide great insight into two primary mechanisms that regulate vessel diameter: shear stress and pericytes. The shear stress simulation method presented here is a useful new tool for analyzing the physical parameters of blood flow *in vitro*. Our results also indicate that imatinib and crenolanib inhibited PDGF signaling and significantly reduced the pericyte coverage of vessels *in vitro*.

Ultimately, the microfluidic system and methods employed in this study have proven useful for understanding the fundamental role of shear stress and pericytes in regulating vessel morphology and provide new means for future research in vascular biology.

Author Contributions

S.E., M.N., K.F., and H.I. performed the experiments and analyzed the data; S.E., M.N., H.I., K.S., Y.N., K.N., T.M., K.F., and R.Y. conceived and designed the project; S.E., K.F., K.S., Y.N., K.N., T.M., and R.Y. wrote the manuscript.

Conflicts of interest

The authors declare that there are no conflicts of interest.

Acknowledgements

The authors thank A. Kubo and M. Moriwake for their assistance in fabricating microfluidic devices, and R. Okada, R. Ueno, R. Banan Sadeghian, Y. Kameda, and Y. Teraoka for valuable discussions. This work was supported by the Core Research for Evolutional Science and Technology (CREST), Japan Science and Technology (JST, Grant Number JPMJCR14W4), and the Japan Agency for Medical Research and Development (AMED). The microfabrication was supported by the Kyoto University Nano Technology Hub.

References

1 S. Morikawa, P. Baluk, T. Kaldoh, A. Haskell, R. K. Jain and D. M. McDonald, Abnormalities in pericytes on blood vessels and endothelial sprouts in tumors, *Am J Pathol*, 2002, **160**, 985-1000.
2 K. De Bock, S. Cauwenberghs and P. Carmeliet, Vessel abnormalization: Another hallmark of cancer? Molecular mechanisms and therapeutic implications, *Curr Opin Genet Dev*, 2011, **21**, 73-79.
3 P. C. Lee, A. N. Salyapongse, G. A. Bragdon, L. I. Shears, II, S. C. Watkins, H. D. J. Edington and T. R. Billiar, Impaired wound healing and angiogenesis in eNOS-deficient mice, *Am J Physiol Heart Circ Physiol*, 1999, **277**, H1600-H1608.
4 M. J. C. Machado, M. G. Watson, A. H. Devlin, M. A. J. Chaplain, S. R. McDougall and C. A. Mitchell, Dynamics of angiogenesis during wound healing: A coupled in vivo and in silico study, *Microcirculation*, 2011, **18**, 183-197.
5 J. W. Wragg, S. Durant, H. M. McGettrick, K. M. Sample, S. Egginton and R. Bicknell, Shear stress regulated gene expression and angiogenesis in vascular endothelium, *Microcirculation*, 2014, **21**, 290-300.
6 J. W. Song and L. L. Munn, Fluid forces control endothelial sprouting. *Proc Natl Acad Sci*, 2011, **108**, 15342-15347.
7 O. Baum, L. Da Silva-Azevedo, G. Willerding, A. Wockel, G. Planitzer, R. Gossrau, A. R. Pries and A. Zakrzewicz, Endothelial NOS is main mediator for shear stress-dependent angiogenesis in skeletal muscle after prazosin administration, *Am J Physiol Heart Circ Physiol*, 2004, **287**, H2300-H2308.
8 M. D. Sweeney, S. Ayyadurai and B. V. Zlokovic, Pericytes of the neurovascular unit: Key functions and signaling pathways, *Nat Neurosci*, 2016, **19**, 771-783.
9 C. Heldin and B. Westermark, Mechanism of action and in vivo role of platelet-derived growth factor, *Physiol Rev*, 1999, **79**, 1283-1316.
10 D. C. Darland, L. J. Massingham, S. R. Smith, E. Piek, M. SaintGeniez and P.A. D'Amore, Pericyte production of cell-associated VEGF is differentiation-dependent and is associated with endothelial survival, *Dev Biol*, 2003, **264**, 275-288.
11 D. Ribatti, B. Nico and E. Crivellato, The role of pericytes in angiogenesis, *Int J Dev Bio*, 2011, **55**, 261-268.
12 J. Fuxe, S. Tabruyn, K. Colton, H. Zaid, A. Adams, P. Baluk, E. Lashnits, T. Morisada, T. Le, S. O'Brien, D. M. Epstein, G. Y. Koh and D. M. McDonald, Pericyte requirement for anti-leak action of angiopoietin-1 and vascular remodeling in sustained inflammation, *Am J Pathol*, 2011, **178**, 2897-2909.
13 A. N. Stratman, K. M. Malotte, R. D. Mahan, M. J. Davis and G. E. Davis, Pericyte recruitment during vasculogenic tube assembly stimulates endothelial basement membrane matrix formation, *Blood*, 2009, **114**, 5091-5101.
14 L. S. Brown, C. G. Foster, J. Courtney, N. E. King, D. W. Howells and B. A. Sutherland, Pericytes and neurovascular function in the healthy and diseased brain, *Front Cell Neurosci*, 2019, **13**, 282.
15 G. Bergers and S. Song, The role of pericytes in blood-vessel formation and maintenance, *Neuro Oncol*, 2005, **7**, 452-464.

16 M. Hellstrom, H. Gerhardt, M. Kalen, X. Li, U. Eriksson, H. Wolburg and C. Betsholtz, Lack of pericytes leads to endothelial hyperplasia and abnormal vascular morphogenesis, *J Cell Biol*, 2001, **153**, 543-553.
17 A. Uemura, M. Ogawa, M. Hirashima, T. Fujiwara, S. Koyama, H. Takagi, Y. Honda, S. J. Wiegand, G. D. Yancopoulos and S. Nishikawa, Recombinant angiopoietin-1 restores higher-order architecture of growing blood vessels in mice in the absence of mural cells, *J Clin Invest*, 2002, **110**, 1619-1628.
18 R. Booth, S. Noh and H. Kim, A multiple-channel, multiple-assay platform for characterization of full-range shear stress effects on vascular endothelial cells, *Lab Chip*, 2014, **14**, 1880-1890.
19 S. Kim, H. Lee, M. Chung and N. L. Jeon, Engineering of functional, perfusable 3D microvascular networks on a chip, *Lab Chip*, 2013, **13**, 1489-1500.
20 Y. Nashimoto, R. Okada, S. Hanada, Y. Arima, K. Nishiyama, T. Miura and R. Yokokawa, Vascularized cancer on a chip: The effect of perfusion on growth and drug delivery of tumor spheroid, *Biomaterials*, 2020, **229**, 119547.
21 M. Campisi, Y. Shin, T. Osaki, C. Hajal, V. Chiono and R. D. Kamm, 3D self-organized microvascular model of the human blood-brain barrier with endothelial cells, pericytes and astrocytes, *Biomaterials*, 2018, **180**, 117-129.
22 J. Kim, M. Chung, S. Kim, D. H. Jo, J. H. Kim and N. L. Jeon, Engineering of a biomimetic pericyte-covered 3D microvascular network, *PLoS One*, 2015, **10**, e0133880.
23 P. Nigro, J. Abe and B. C. Berk, Flow shear stress and atherosclerosis: A matter of site specificity, *Antioxid Redox Signal*, 2011, **15**, 1405-1414.
24 P. Carmeliet, Angiogenesis in life, disease and medicine. *Nature*, 2005, **438**, 932-936.
25 J. Almaca, J. Weitz, R. Rodriguez-Diaz, E. Pereira and A. Caicedo, The pericyte of the pancreatic islet regulates capillary diameter and local blood flow, *Cell Metab*, 2018, **27**, 630-644.
26 K. Kato, R. Diéguez-Hurtado, D. Y. Park, S. P. Hong, S. Kato-Azuma, S. Adams, M. Stehling, B. Trappmann, J. L. Wrana, G. Y. Koh and R. H. Adams, Pulmonary pericytes regulate lung morphogenesis, *Nat. Commun*, 2018, **9**, 2448.
27 J. Ruan, M. Luo, C. Wan, L. Fan, S. N. Yang, M. Cardenas, H. Geng, J. P. Leonard, A. Melnick, L. Cerchietti and K. A. Hajjar, Imatinib disrupts lymphoma angiogenesis by targeting vascular pericytes, *Blood*, 2013, **121**, 5192-5202.
28 O. Melaiu, C. Catalano, C. De Santi, M. Cipollini, G. Figlioli, L. Pelle, E. Barone, M. Evangelista, A. Guazzelli, L. Boldrini, E. Sensi, A. Bonotti, R. Foddis, A. Cristaudo, L. Mutti, G. Fontanini, F. Gemignani and S. Landi, Inhibition of the platelet-derived growth factor receptor beta (PDGFRB) using gene silencing, crenolanib besylate, or imatinib mesylate hampers the malignant phenotype of mesothelioma cell lines, *Genes Cancer*, 2017, **8**, 438-452.
29 G. Chouinard-Pelletier, E. D. Jahnsen and E. A. V. Jones, Increased shear stress inhibits angiogenesis in veins and not arteries during vascular development, *Angiogenesis*, 2013, **16**, 71-83.
30 P. A. Galie, D.-H. T. Nguyen, C. K. Choi, D. M. Cohen, P. A. Janmey and C. S. Chen, Fluid shear stress threshold regulates angiogenic sprouting, *Proc. Natl. Acad. Sci. U. S. A.*, 2014, **111**, 7968–7973.
31 J. W. Song and L. L. Munn, Fluid forces control endothelial sprouting, *Proc. Natl. Acad. Sci. U. S. A.*, 2011, **108**, 15342–15347.
32 H. Kang, K. J. Bayless, and R. Kaunas, Fluid shear stress modulates endothelial cell invasion into three-dimensional collagen matrices, *Am. J. Physiol. Heart Circ. Physiol.*, 2008, **295**, 2087–2097.
33 M. A. Winkelman, D. Y. Kim, S. Kakarla, A. Grath, N. Silvia and G. Dai, Interstitial flow enhances formation, connectivity, and function of 3d brain microvascular networks generated within microfluidic device, *Lab Chip*, 2021, **22**, 170–192.
34 C. G. M. van Dijk, M. M. Brandt, N. Poulis, J. Anten, M. van der Moolen, L. Kramer, E. F. G. A. Homburg, L. Louzao-Martinez, J. Pei, M. M. Krebber, B. W. M. van Balkom, P. de Graaf, D. J. Duncker, M. C. Verhaar, R. Luttge and C. Cheng, A new microfluidic model that allows monitoring of complex vascular structures and cell interactions in a 3D biological matrix, *Lab Chip*, 2020, **20**, 1827–1844.
35 S. Kim, J. Chen, T. Cheng, A. Gindulyte, J. He, S. He, Q. Li, B. A. Shoemaker, P. A. Thiessen, B. Yu, L. Zaslavsky, J. Zhang and E. E. Bolton, PubChem in 2021: new data content and improved web interfaces, *Nucleic Acids Res.*, 2021, **49**, D1388–D1395.
36 1 T. Cheng, Y. Zhao, X. Li, F. Lin, Y. Xu, X. Zhang, Y. Li, R. Wang and L. Lai, Computation of octanol-water partition coefficients by guiding an additive model with knowledge, *J. Chem. Inf. Model.*, 2007, **47**, 2140–2148.
37 M. R. Owen, T. Alarcon, P. K. Maini and H. M. Byrne, Angiogenesis and vascular remodeling in normal and cancerous tissues, *J Math Biol*, 2009, **58**, 689-721.
38 M. A. J. Chaplain, S. R. McDougall and A. R. A. Anderson, Mathematical modeling of tumor-induced angiogenesis, *Annu Rev Biomed Eng*, 2006, **8**, 233-257.
39 S. Ichioka, M. Shibata, K. Kosaki, Y. Sato, K. Harii and A. Kamiya, Effects of shear stress on wound-healing angiogenesis in the rabbit ear chamber, *J Surg Res*, 1997, **72**, 29-35.
40 C. M. Peppiatt, C. Howarth, P. Mobbs and D. Attwell, Bidirectional control of CNS capillary diameter by pericytes, *Nature*, 2006, **443**, 700-704.
41 C. N. Hall, C. Reynell, B. Gesslein, N. B. Hamilton, A. Mishra, B. A. Sutherland, F. M. O'Farrell, A. M. Buchan, M. Lauritzen and D. Attwell, Capillary pericytes regulate cerebral blood flow in health and disease, *Nature*, 2014, **508**, 55-70.
42 W. Cai, H. Liu, J. Zhao, L. Y. Chen, J. Chen, Z. Lu and X. Hu, Pericytes in brain injury and repair after ischemic stroke, *Transl Stroke Res*, 2017, **8**, 107-121.
43 J. Gautam and Y. Yao, Roles of pericytes in stroke pathogenesis, *Cell Transplant*, 2018, **27**, 1798-1808.